1 TITLE PAGE

Electrochemical Hydrogen Compressor

DOE Grant DE-FG02-05ER84220
Analytic Power Contract C104

May, 2006

FINAL REPORT
by
Brian S. MacKenzie and David P. Bloomfield (PI)

Analytic Power Corp.
1109 Sangre de Cristo
Santa Fe, NM 87501

2 EXECUTIVE SUMMARY

The research performed will lead to a commercial electrochemical hydrogen compressor. While our research did not completely investigate Molybdenum as a hydrogen anode or cathode, it did show that etched 316 stainless steel is inadequate for an EHC. It also showed that molybdenum bipolar plates, photochemical etching processes, and Gortex Teflon seals are too costly for a commercial EHC. The use of carbon paper in combination with a perforated thin metal electrode demonstrated adequate anode support strength, but is suspect in promoting galvanic corrosion. The nature of the corrosion mechanisms are not well understood, but locally high potentials within the unit cell package are probably involved. The program produced a design with an extraordinary high cell pitch, and a very low part count. This is one of the promising aspects of the redesigned EHC. The development and successful demonstration of the hydraulic cathode is also important. The problem of corrosion resistant metal bipolar plates is vital to the development of an inexpensive, commercial PEM fuel cell. Our research suggests that there is more to the corrosion process in fuel cells and electrochemical compressors than simple, steady state, galvanic stability. It is an important area for scientific investigation.

Table of Contents

List of Figures

List of Tables

3 GOALS VS ACCOMPLISHMENTS

The Phase I objectives were not completely met:

Objective	Value	Accomplished
Demonstrate performance	.4 V/cell @ 1 amp/cm2	0.215 V@ 391amp/cm2
Demonstrate cell sealing	to 2000 psia.	Completed
Demonstrate pressure ratio	at least 100	11.7
Operate the anode on dry H2		Completed
Operate hydraulic cathode		Completed
Design for min. shunt current		Excessive Corrosion

4 SUMMARY

The Electrochemical Hydrogen Compressor EHC was evaluated against DOE applications for compressing hydrogen at automobile filling stations, in future hydrogen pipelines and as a commercial replacement for conventional diaphragm hydrogen compressors. It was also evaluated as a modular replacement for the compressors used in petrochemical refineries. If the EHC can be made inexpensive, reliable and long lived then it can satisfy all these applications save pipelines where the requirements for precious metals exceed the world production.

The experiments and analysis conducted under the program lead to several recommended future research directions. :First, we need a better understanding of the Corrosion mechanisms involved. The first recommendation must be into improved diagnosis of experimental cells with titration to diagnose loss of membrane active sites.
We suspect the corrosion includes Galvanic mechanisms. The experiments conducted pointed to locally high potentials. The mechanisms involved in this phenomenon are poorly understood. Shunt currents at hydraulic cathode ports appear to be problematic. In addition to corrosion phenomena there is evidence of high component resistivity. This may be due to the deposition of simple organic compounds which may be produced electrochemically on the surface of the metal support screens which contact carbon. An analytic investigation is warranted of possible electro-organic sythesis mechanisms with emphasis on oxalates formation. The simple diagnostic of placing the contaminated parts in an oxidizing atmosphere at high temperature and observing the weight loss can be performed simply and would reveal the existence of organic compounds. Investigation into the effects of conductivity enhancers such as carbon microlayers on supporting carbon paper is needed.

A few corrosion solutions should be investigated such as surface passivation of 316 SS parts using nitric acid. Ultra thin silane/siloxane polymer coatings should be tried. These may be especially useful in conjunction with metal felt replacement of carbon paper. A simple cure for the very high, localized corrosion of the anode might be to diffusion bond the metal electrode support screen to bipolar plate. This will insure uniform resistance perpendicular to the plane of the cell and eliminate some of the dependence of the resistance on high stack compression.

Alternative materials should be explored. Alternatives to carbon in the cell are likely to be helpful in any context. In particular, alternatives to carbon paper GDLs such as metal felts and alternatives to carbon supports for Pt such as TiC and TiB2 might also be worthwhile and would also be helpful to fuel cells as well. Some alternative to the metals used in the cell such as Mo and 316 SS are potentially useful. The investigation of Al/Mg/Si alloys in particular is suggested. In addition, corrosion resistant materials such as Nb and Mo might prove useful as cladding materials that can be hot stamped.

There are several areas in cost reduction that should be fully explored The first of these is the use of the pressure washers tpe water pumps. The power consumption of these pumps is a concern, but their cost is surprisingly low Two components of unit cell construction are extremely costly. The first of these is the photoetching process, where. selective etching of alloys present a different composition in the cell. An alternative to photoetching may be hot stamping. An investigation of materials for hot stamping and the dimension tolerance attainable with this process is first on the agenda. Hot stamping of clad materials should also be studied. Photoetched electrode supports can be replaced with expanded metal screens (Dexmet). Another high cost area is the use of Gortex TFE seals. Analytic's prior experience with Acrylic seals shows they can replace TFE.

4.1 Original Hypothesis,

Analytic Power proposed to design, build and test a single cell of an electrochemical hydrogen compressor (EHC). Significant weight, volume, and cost savings were expected compared to conventional low flow, high pressure ratio (diaphragm) compressors. A significant power input reduction was expected because electrochemical compressor operation is isothermal, whereas the conventional compressor is a multistage, intercooled, isentropic device. Electrochemical compressors are simpler, having no moving parts. This feature makes an EHC very attractive for applications where reliable components are critical to insure long system life.

Analytic Power built electrochemical compressors that attained 1000 psi (oxygen) and 2000 psi (hydrogen). They exhibited relatively high performance degradation rates attributable to two problems anode flooding and component oxidation. The source of the problem was twofold. First, the anode support structure, used a 0.25 in thick, sintered titanium support, which was nitrided for corrosion resistance. This component filled with water, blocking hydrogen from reaching the anode, and oxidation of several of the compressor components, including the nitrided titanium anode support.

4.2 Approach

Analytic's proposed approach was to redesign the unit cell incorporating several revolutionary changes. With the design complete we built and tested the single cell component of the EHC. Our objectives were to reduce the part count, increase the pitch

and, hopefully, lower the cost. We also tried more corrosion resistant materials. This section discusses the new design and compares it to the original.

4.2.1 Configuration

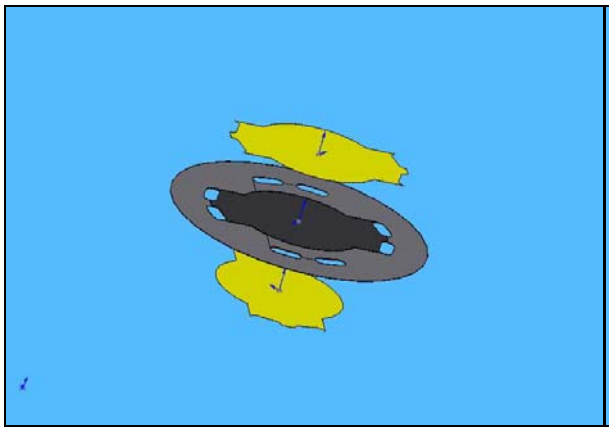

Figure 1 New Cell Pack 3 parts per cell

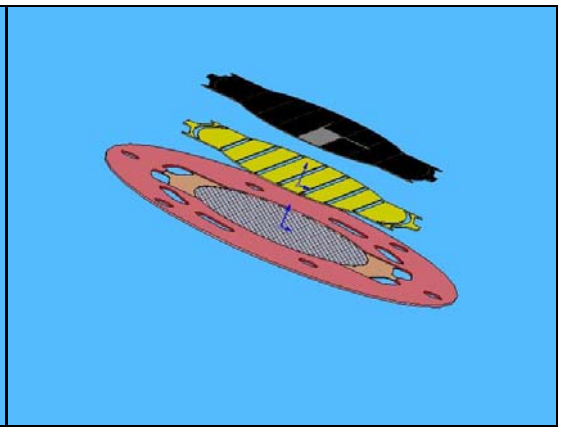

Figure 2 Old Cell pack 4 parts per An

4 parts per Cathode, 3 parts cooler (not shown)

Figure 1 shows an exploded view comparisons of the old and new designs. Figure 2 shows the old anode and cathode design. The old design had 6 manifolds, 2 each for anode reactant, high pressure cathode and cooler. The new design integrates the cooler and cathode compartments and is a 90 degree crossflow design. The cooler section is not shown in the figure, but it used a separate bipolar plate and the same flow fields as the other compartments. There are eleven parts in the original unit cell.

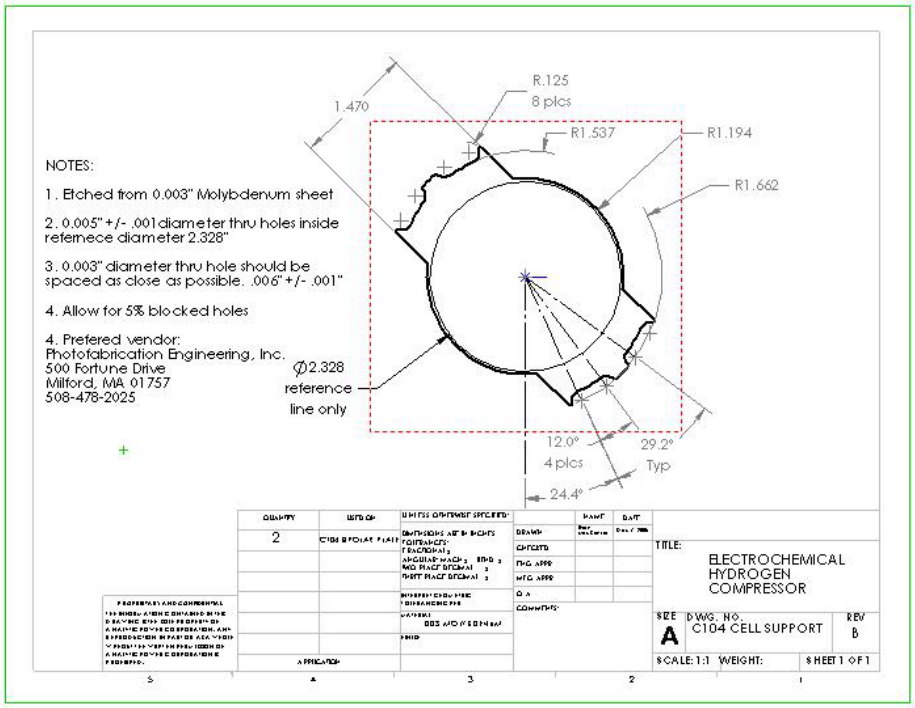

Figure 3 Electrode support screen

The new design has three components for the anode, and hydraulic cathode, reducing the cell components by eight parts. Figure 1 shows the new bipolar plate design

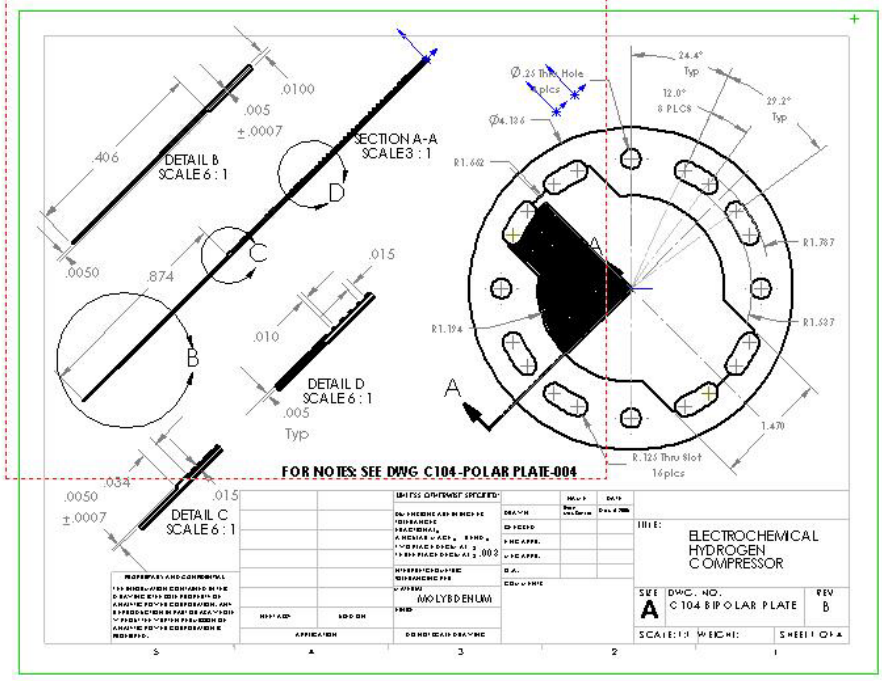

Figure 4 Bipolar Plate Drawing showing revised flow field configuration

and the two electrode support structures. Because there are fewer components there are fewer sealing surfaces and the number of gaskets per cell is reduced by four. The original design required separate current collectors, whereas the new design incorporated the current collector in the cell plate further reducing the number of components. The total reduction in components per cell pack (11 cell hardware, 4 gasket and 2 current collectors) is seventeen. The cell pack thickness is reduced by 78% where the old cell packet was 0.155 inches and the new, 0.034 inches. The new bipolar plate is only .027 inches thick and the cell is .007 inches. The result is a simplified design with a cost saving and a decrease in the cell contact resistance due to the reduction of components and contact. The new EHC design potentially decreases the weight, volume, cost, resistance, and input power.

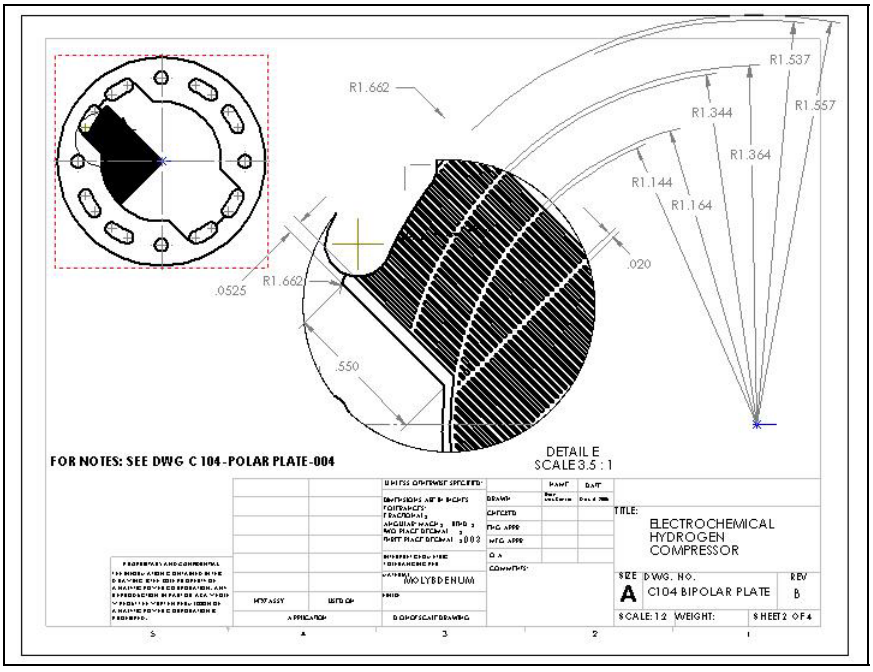

Figure 5 Drawing detail of bipolar platge flow field

4.2.1.1 *Bipolar Plate Redesign*

The bipolar plate is the key to the new design. Rather than incorporate the flowfields into separate structures as in the original design, the new design etched the flow field grooves and surrounding seal area into the plate

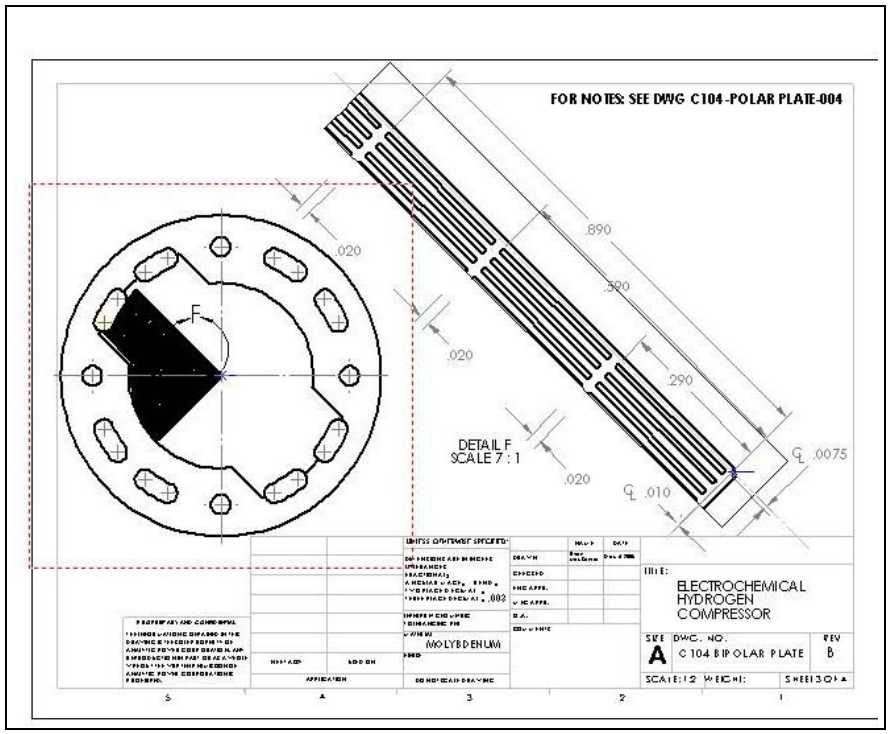

Figure 6 Bipolar plate flow field details

material – on both sides of the plate. The bipolar plate accommodates the seal and the flow field grooves. Adjustments to material thickness and dimensions were required due to material availability and limitations of the etching process. The bi-polar Plate thickness was reduced to .015" due to material availability. The flow channels were increased from .010" wide to .015" wide with the space between the channels increased from .005 to .010. The cell support structure was supposed be .003" Molybdenum. The tolerance is plus or minus .003" and .0007" for the height of the gasket area. PO's were issued with Photofabrication Engineering Inc, with an estimated delivery time of mid January. Cost of the Bi-polar plates is $1,850 and the cell support is $1,260. We ordered both Molybdenum and SS bipolar plates. The molybdenum cell support structures were never made and the molybdenum bipolar plates were delivered after the contract expired. The stainless steel parts were delivered in mid February and early March.

Figure 6 shows a detailed drawing of the electrode support screens that are used on each side of the cell. We originally planned to have these fabricated from photoetched molybdenum,

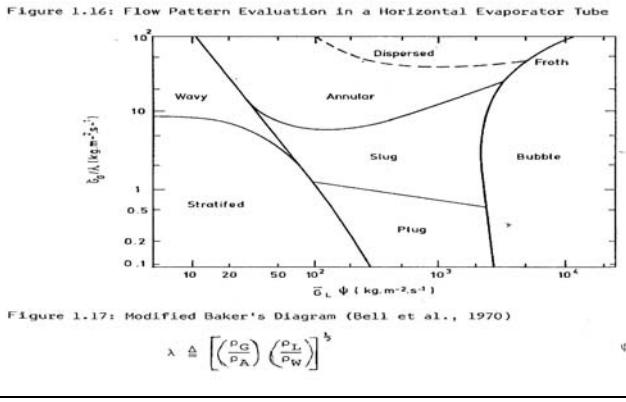

Figure 7 Baker Plot of two phase flow regimes

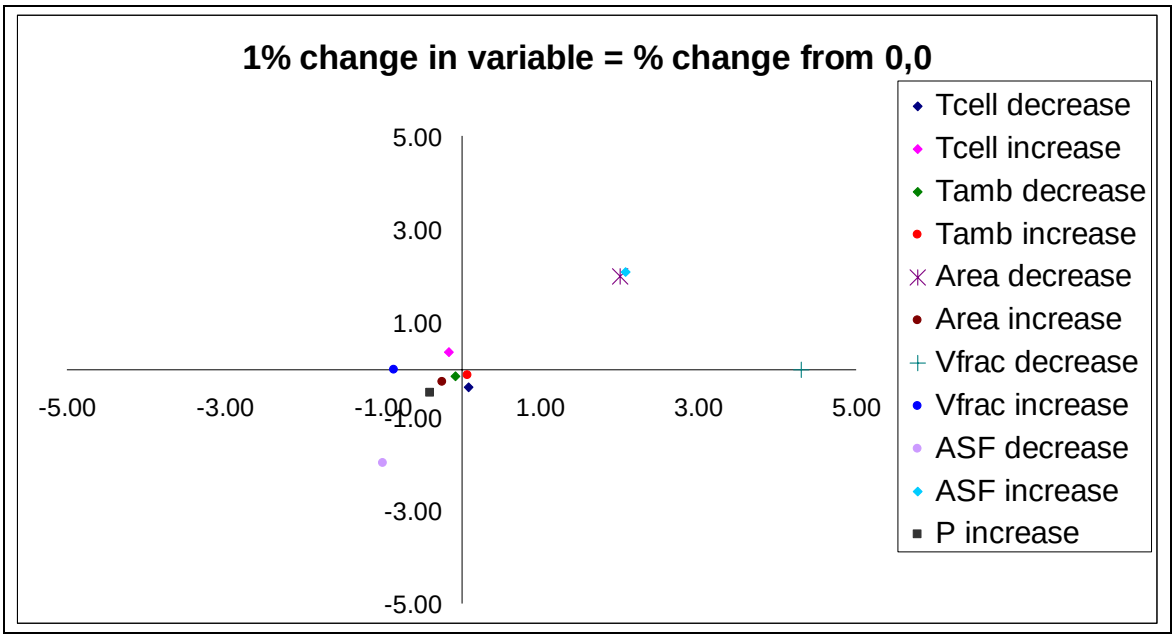

Figure 8 Baker diagram Movement

which is corrosion resistant. It was found that the larger diameter holes required by the etching process permitted extrusion of the cell under high cell pressure. We then interposed carbon paper GDLs between the electrode and the support screen. The bipolar plate overall drawing is shown in Figure 4 and drawings showing the details of the flow fields which are etched into the bipolar plate surface are shown in Figure 5 and **Error! Reference source not found.**. The channel size (.010" wide x .005" deep with .005" between channels) and the height of the flow field, 0.085 inches and overall thickness of 0.027". The channel dimensions provide 66% open area. However, the 0.001" metal cell support reduces this to 33%. Considerable attention to detail is required when designing the flow fields for a circular cell so as to avoid short cuts for fluids flowing through the cell.

Table 1 Design Parameters

Description	Value
Void fraction	0.15
H2 flow rate =	4.68E-02
H20 flow rate	2.65E-01 l/hr or 2.37E-03 l/hr per cell
Pressure	2500psi
Cell Temperature	160F
Number of channels	112 channels @ 2.95in average length
Channel width	0.010
Channel depth	0.005
Distance between channels	0.005
ASF	350
Re	2.76
h	13.25 W/m^2K
Nu	1.47
DP	8.7E-04 psi / channel or .12 psi / cell

4.2.1.2 Fluid Flow

The new flow field pressure drop vs flow properties were calculated. The cross flow

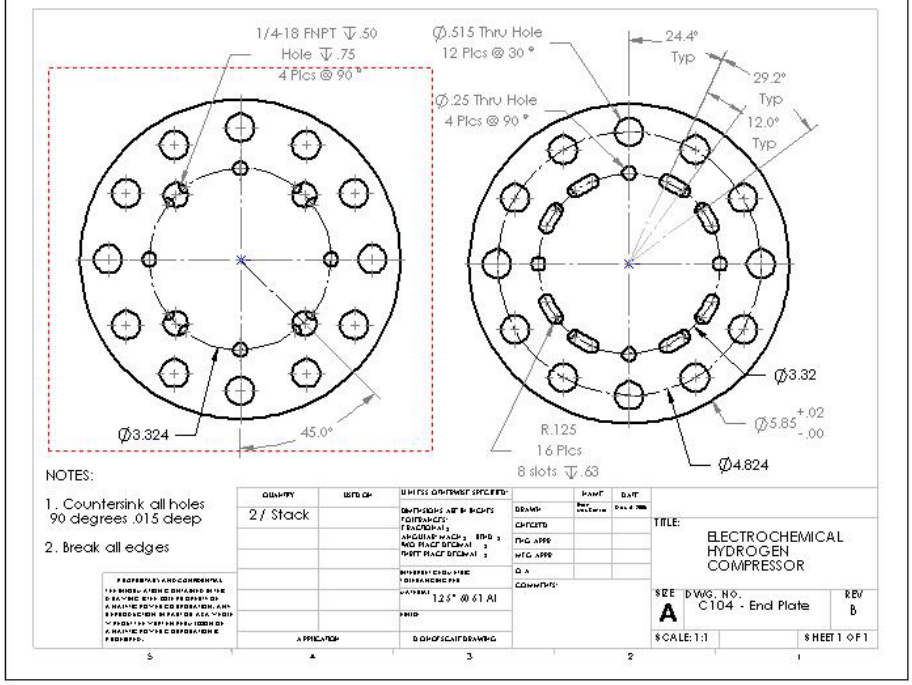

Figure 9 End Plate Drawing

design was used to strengthen the loaded parts and preclude crossover. The pressure drop per cell is .12 psi. The design parameters are shown in Table 1. One of the design issues is that the active area exposed to reactant hydrogen is reduced to 25% because of the perforated metal electrode support screen. We investigating using a porous metal support which can be manufactured to less than .005 thick and with up to 80% open area. The problem is that it is not available in corrosion resistant materials.

The channel size was determined with a sensitivity study of pressure drop vs hydrogen void fraction in the Cathode. A design requirement was to maintain a flow in the "bubble range" according to the Baker diagram shown Figure 7. The baker diagram shows several flow regimes for two-phase flow. Because of the many variable involved in determining location on the Baker diagram f(Tcell, Tamb, Pressure, ASF, Void Fraction, and Channel Area) a spread sheet was constructed to determine movement on the Baker diagram as a function of each of these parameters. The chart in Figure 8 shows the change in the location on the baker diagram as a function of a change of 1% of each on the parameters individually. For instance, a 1% decrease in the Channel Area results in a movement along the baker diagram of 1.5% on the x and 1.5% on the y axis.

Figure 8 shows it is possible to determine movement on the Baker chart. In our case we were on the border of plug flow and bubble flow. So the void fraction was decreased to 0.15 from 0.30, the channel depth was reduced to 0.005 from 0.010, and a higher current density of 350 a/cm^2 compared to 300 was selected based on expected improved performance from design changes that will reduce contact resistance, discussed later in this report. The design parameters selected are shown in Table 1

4.2.2 Hardware Design

This section covers the design for the remaining stack hardware. This includes the follow up system (endplate and tie rods), gaskets, current collector, insulator, and spider. Parts were ordered Dec 14 from Best Machining with an estimated delivery time of Dec. 30.

The Follow-up system is the system of end plates current collectors, insulators and tie rods that together keep the stack in compression. It is designed so the cells are subject to a planar compressing force that minimizes contact

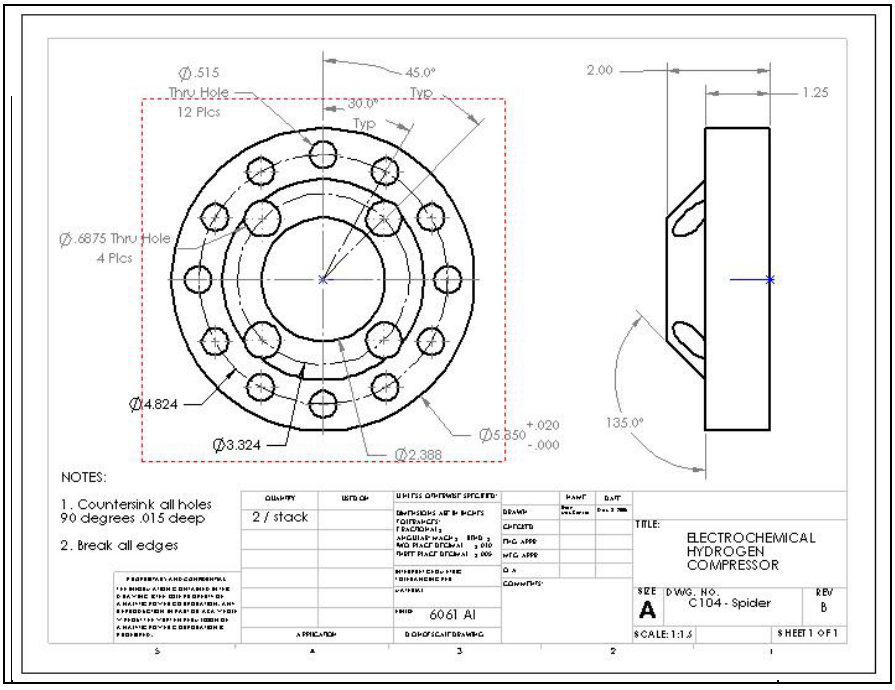

Figure 11 Cell Stack System Spider Conductor

Table 2 Tie Rod Calculations (Cont.)

Calculate Bolt area as a function of Force on bolts, factor of safety and # of bolts					
EQUATIONS	F(bolts) P *(Ai + Ag *m)			42759.2	lb
	Sigma(bolts) Sigma(ult) / FS			20200	psi
RESULTS	sigma(bolts) F(bolts)/A(stress) *1/n				
	A(Stress) FS Sigma(ult) / Sigma(bolts)			0.176	in^2
	FS yield Sigma(yield-bolts) / Sigma (bolts)				1.75
	F(bolts) force on bolts				
KNOWNS / INPUTS	Sigma(bolts) Stress on bolts				
	A(Stress) stress area of bolts				
Calculated A(Stress)	n number of bolts	0.1764			
Select Bolt Size	KNOWNS / INPUTS	0.5625		9/16 - 12UNC-2A	
Actual A(Stress) of selected bolt	Factor of Safety		5	0.226	Table 5-1: machine elements
	n number of bolts		12		
W=Calculated Clamping force	Sigma(ult - bolts)	42759.28	101000	psi	
u=Friction Coefficient	Sigma(yield - bolts)	0.15	35500		pg 313: Machine elements
rod diameter		0.5625			
Coef. Tightening Torque		0.195			Pg 313: Machine elements
RESULTS					
T	390.8465	ft lbf			
Sigma (bolts) F (bolts)/A (stress) *1/n				15766.69	
FS Sigma(ult) / Sigma(bolts)				6.40	
FS yield Sigma(yield-bolts) / Sigma (bolts)				2.25	

resistance between cell parts and maintains the correct sealing force on the stack – or in the present case, the test fixture. A two part end plate is used. The endplate proper,

Table 4 Gasket Calculations

Calculate Gasket loading (yield value)					
EQUATIONS					
	F(gasket) Ag * q				
	q [P *(Ai + Ag * m)] / Ag				
	F(bolts) P * (Ai + Ag * m)				
	F(gasket) Gasket Contact Pressure				
	q Pressure acting on Gasket due to bolts				
	P Maximum operating pressure				
	Ai Area under Pressure				
	Ag Effective Gasket Area				
	m Gasket factor (assumed to be 1, for soft rubber				
	Where, m ratio of (contact pressure / fluid pressure)				
KNOWNS / INPUTS					
	Diameter	in		Area	in^2
	D1	2.388		A1	4.478768
4.822	D4	4.26		A4	14.25309
	Sigma(yield - Gasket)		3500		
	P		3000	psi	
	m		1		
	Ai A1		4.47	in^2	
	Ag (A2 - A1) + (A4 - A3)				
	Ag	9.774324	in^2	(calc by equation above)	
	q	4374.653	psi		
	F(gasket)	42759.28	lb		
	F(bolts)	42759.28	lb		
NOTE:	Fg must be > Fb				
	Sigma(yield - gasket) < q for gasket to seal				
RESULTS					
		Gasket will seal			
		Fg is =>Fb			

Figure 9, is in contact with an insulator and current collector, Figure 10, and has a flat compression surface. It is drilled and tapped to provide reactant gas access to the cell manifolds. It also has tie rod holes that are drilled slightly larger than the tie rod diameters. The “spider” is a circular plate whose lower surface is tapered so as to contact the end plate over an area equal in diameter to the cells active area. The reason for this is that when the cathode gas pressure is developed, the end plate tends to deform at the centerline of the stack. If such a deflection is permitted to take place then the centerline of the stack would become “unloaded.” The spider applies a restoring force to maintain the endplate flat under the stress of the high cathode pressure.

4.2.2.1 Compression Loading

The calculations for sizing the tie rods which hold the stack in compression are shown in Table 2 and Table 3. The tables show the calculations for the bolt stress and torque.

With a factor of safety of 5, and 12 bolts the bolt size requires a stress area of 0.18 inches. The tables show the equations used to determine stress area. The bolt size selected is 9/16 - 12UNC-2A which has a stress area of 0.266 inches. Therefore the factor of safety is 6.4 or 2.25 when compared to the yield strength of the bolts. The required bolt torque is 390 ft lbf.

4.2.2.2 Gasket Design

The as received gasket, microporous TFE, showed compression vs. deflection (Figure 13) diagram of slightly thicker gasketing material. In order to seal, the gasket must deflect 60-65%. Testing on the .019 inch samples exhibitied this deflection. The frames were modified and reduced an additional .004 - .006 inches. The gasket seal pressure is calculated to be 4,375psi and the bolt force required is 42,759lb. A spread sheet was created to determine bolts stress area based on Factor of Safety (FS) and the number of bolts used. We used 12 bolts of 9/16 - 12UNC-2A. This gives us a FS = 6.4 and 2.25 based on Ultimate and yield stress respectively. Table 4 shows the equations used to determine required for gaskets seal load.

Table 5 Baseline cost 4cfm compressor @0.5 a/cm2

4CFM (4 Stacks 0.5 A/cm2)	Baseline No. Parts	Cost each	Total
Cells	974	$ 3.41	$ 3,323
Bipolar Plates SS	974	$ 14.27	$ 13,899
Electrode Support SS	1948	$ 3.24	$ 6,312
Seals 4.14" OD 0.5 mm	1948	$ 7.50	$ 14,610
Follow Up System (set)	4	$ 1,190.00	$ 4,760
			$ 42,903

4.2.3 Economics

The manufactured EHC costs were developed for several commercial applications from 4 to 14 CFM application for replacing conventional diaphragm compressors. The design and cost targets were supplied by

Table 6 EHC Cost breakdown @1 amp/cm2

4 CFM (1 stack 1A/cm2)	No. Parts	Cost Each	Total
Cells	487	$ 3.41	$ 1,661
Bipolar Plates	487	$ 14.27	$ 6,949
Electrode Support	974	$ 3.24	$ 3,156
Seals 4.14" OD 0.5 mm	974	$ 7.50	$ 7,305
Follow Up System (set)	2	$ 1,190.00	$ 2,380
			$ 21,452

Pressure Products Industries. A projected cost breakdown of the EHC stack is given in. Table 5. The design assumes the 2.5 in diameter cells being tested now. The cost of the MEA in a low volume application such as this, are estimated to be 100$/ft2. It was found that the cost of molybdenum parts were an order of magnitude higher than stainless steel parts. based on quotes from the manufacturers. The table shows that a 4 stack system operating at 0.5 amp/cm2 would cost about $42,900. This is about 1.8 times the cost of a conventional 4CFM compressor. If the compressor can run at 1 amp/cm2, then the EHC cost is cut by half. The cost of the EHC is then about 90% of the cost of a conventional compressor. However this leaves no funding for BOP. Increasing the cell diameter has a relatively minor effect on the system cost. The most expensive part in the Baseline case of Table 6 is Teflon seals. If in addition to operating at high current density, the seals are eliminated or replaced with inexpensive acrylic seals, the compressor cost will drop to $14,150. This is only 59% of the diaphragm compressor cost and leaves room for BOP expenses.

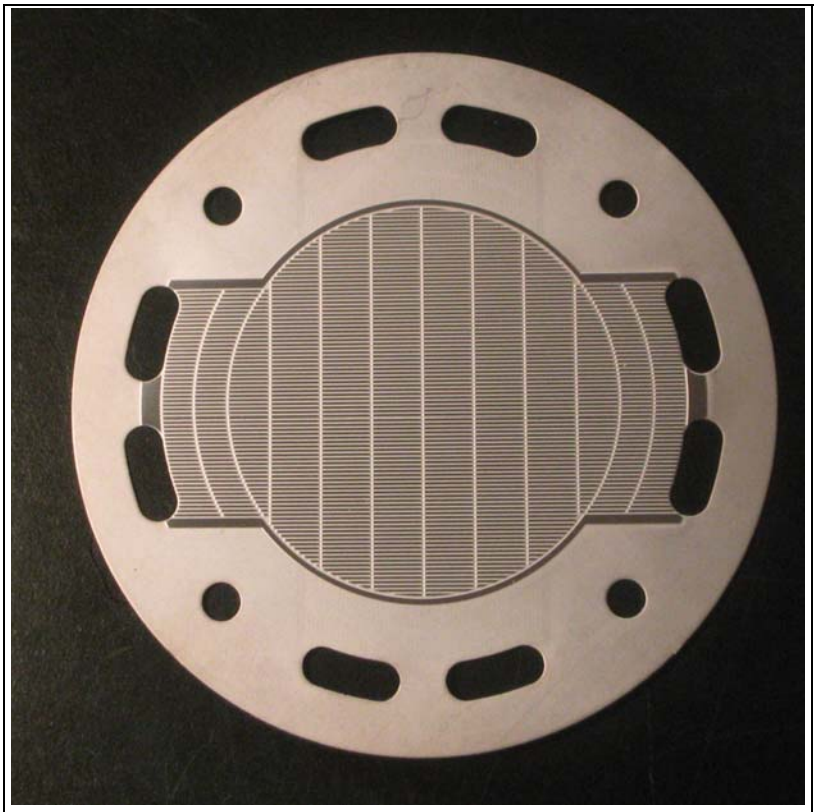

Figure 12 Stainless Steel Bipolar Plate showing etched flow fields and Ports

We have received the MEA's from Ion Power. We intended to experiment with three thicknesses (.011, .015, .017 in) of the same loading (Catalyzed 0.5mg Pt/cm2/side). Based on the strength of a carbon paper supported GDL and a metal screen electrode support, the 0.011 material is adequate.

4.2.4 Materials selection

The screen material corrosion properties are important. Surprisingly, it was discovered that if the hydrogen anode is kept below 400mv (SHE), silver might be a reasonable metal to use. Designing a system that excludes air from the cell at all times and maintains a reducing environment is not an easy task. Because silver is a known hydrogen redox catalyst, such an approach would result in a very lost cost cell. We queried several metal supply companies to determine whether stainless steels might be stable in the EHS. The

stainless steel flow fields in the USMC program appeared to be corrosion resistant at the low electrode potentials. Nb and Mo candidate materials for the Exmet screen are too brittle to obtain in wire or felt form. The flow fields in Figure 12 were fabricated by photoetching..

We did consider a sintered titanium cell support on the anode side of the cell with a screen stack using progressively increasing pore sizes. Sintered Ti is generally very expensive and an anisotropic pore size would have been even more expensive, if it could be done at all. Adjacent to the cell one would use the smallest pore opening possible. Titanium, unfortunately, is oxidized by water and the TiO_2 layer formed is not conductive. Prior work with this material shows that the TiN coatings used to protect Titanium plates also oxidizes in the cell environment. The material for an electrode support screen could be either molybdenum or niobium expanded metal. Both Christine Zawodzinski (LANL) and A. Laconti (Giner Inc) thought that these were the best materials for use adjacent to the cell catalyst. A quote was obtained from Delker for Niobium Screen. We specified a photoetched molybdenum to get a smaller mean pore size than the Dexmet material which has a length along the diamond of 20 mils and a strand width of 3 mils. This might be superior to the photoetched material we wound up using.

Photoetching is too costly a process for forming bipolar plates. Molybdenum is also too costly a material for use in this application. Bipolar plate materials such as Al/Mg/Si alloys and polymer coated material should be studied. Future research should also concentrate on expanded metal screen electrode supports and metal felt GDLs. The metal felts might be effectively coated with imide or siloxane polymers. This requires experimental proof.

4.2.4.1 Gasket Material Selection

Table 7 Expanded metal screen alternative

Dexmet Product Code	1.3NB3-020F	5NB5-031F	10NB10-050F
Base Metal Thickness	0.0013 inch	0.005 inch	0.010 inch
Material	Niobium	Niobium	Niobium
Strand Width	0.003 inch	0.005 inch	0.010 inch
LWD	0.020 inch	0.031 inch	0.050 inch
Open area	50%	50%	31%

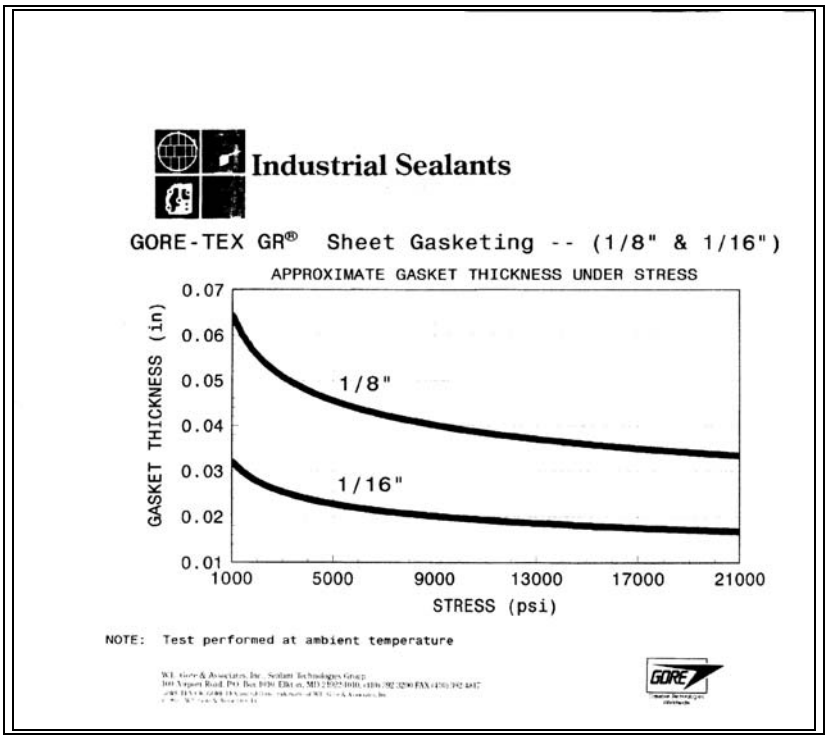

Figure 13: Compression vs. deflection: Goretex GR Gasketing

Gasket material was received for both .040 and .020 inch thick GORE-TEX GR Sheet. However, they were unable to supply a compression vs deflection chart for these thicknesses (See Figure 13). However, they provided one for both 1/8" and 1/16" material. From this chart both these thicknesses show a reduction to 35-40% of total thickness at our expected compression of approx. 5,000psi. We have designed the plates by assuming a size reduction to 60% of starting thickness not 30-40%. Therefore, we needed additional testing on the gasketing material in house. If the samples provided act similarly we would expect a finish thickness of .006-.008 inches. We had been designing at .010 inches. While the Goretex product is a superior sealing material, it is far too expensive to be used in an EHC. It is possible to use acrylics in the EHC.

4.2.4.2 MEA

MEA's were received from Ion Power. The first tests inidicated that the catalyst layers might be unstable in the hydraulic cathode. Testing outside the cell indicated that the catalyst

Table 8 Test Stand Design Parameters

Cell	Value	Units	Heat	Value	Units
Diameter	2.32	in	Vi	0.0622	volts
Area	27.266	cm2	Polarization	0.219	v/a/cm2
Current Density	2000	ma/cm2	Pideal	3.39	watt
Current	54.53	amp	Ptotal	27.27	watt
Volts	0.50	volt	Heat	23.87	watt
Power	27.27	watts	temp rise	20	F
			Cp	1	Btu/hr F
Anode			wH2O	0.513	gm/sec
nH2,c	0.000283	gmol/sec	vH2O	0.308	lpm
wH2,c	0.000565	gm/sec	Void Fraction	0.9%	
vH2,c	0.380	SLPM			
UH2	70%				
nH2,in	0.000404	gmol/sec			
WH2,in	0.000807	gm/sec			
vH2,in	0.542	SLPM			
Cathode H2			Cathode Water		
Press	2000	psi	Void Fraction	10%	10%
Press	136	atm	Dens H2 (1 at	0.004900	lbm/ft3
nH2	0.000283	gmol/sec	SPG (1atm)	0.000079	
wH2	0.000565	gm/sec	SPG H2 (Cath	0.010684	
vH2	0.002791	LPM	vH2O	0.025120	LPM

layer was stable. Future tests should check this compatibility further to see if there is an interaction of the hardware with the catalyst layer.

4.2.5 Test Stand

The test stand flow schematic is shown in Figure 36. The numbered nodes correspond to nodes in the simulation program written for the test stand. Changes to the original USMC configuration are required by the integration of the cathode and cooling loop. The integrated loop has the following advantages:

- Ensures water distribution in the EHC membrane.
- Permits the use of dry hydrogen on the anode side.
- Reduced stack part count.

In addition, the presence of liquid water, especially if it is diluted with solute, will promote the osmotic pumping of anode liquid water to the cathode side.

The design parameters used for developing the test stand are shown in Table 8.The use of liquid water on the cathode side requires a very high pressure water pump to circulate the water throughout the cathode system. The pressure drop in the system is not expected to be very high, although the two phase nature of the flow (hydrogen/water) will increase the pressure drop compared to a single phase. The important requirement is that the pump housing and seals be able to withstand very high pressures. Fortunately, the development of "pressure washing" has made high pressure, inexpensive water pumps available. These pumps can produce up to 5000 PSI. They are very high capacity, over an order of magnitude higher than the EHC single cell. But the costs are ~$250 to $500 for a complete, reconditioned unit. Problems were anticipated in the development of the water separator. The completed test stand is shown in Figure 14 and Figure 15

Figure 14 Completed Test Stand - Front View

4.3 Resolving prior problems

4.3.1 Hydraulic cathode.

The hydraulic cathode is filled with circulating cooling water. Cooling and humidification of the cell is accomplished from the cathode side, eliminating a separate cooling compartment. The problem of suppressing corrosion using water is no more difficult with the hydraulic cathode than the separate cooling supply approach. The principle concern is to minimize shunt currents. Additionally, solutes such as sugar can be added to the cathode water to create a concentration gradient that drives any water formed in the anode compartment to the cathode. High pressure hydrogen simply bubbles into the cathode cooling water and is simple to separate. Because of the hydration of the membrane from the cathode side, dry hydrogen can be used at the anode. In most commercial applications, hydrogen is purified by a PSA unit which supplies dry hydrogen at 100 to 200 PSI.

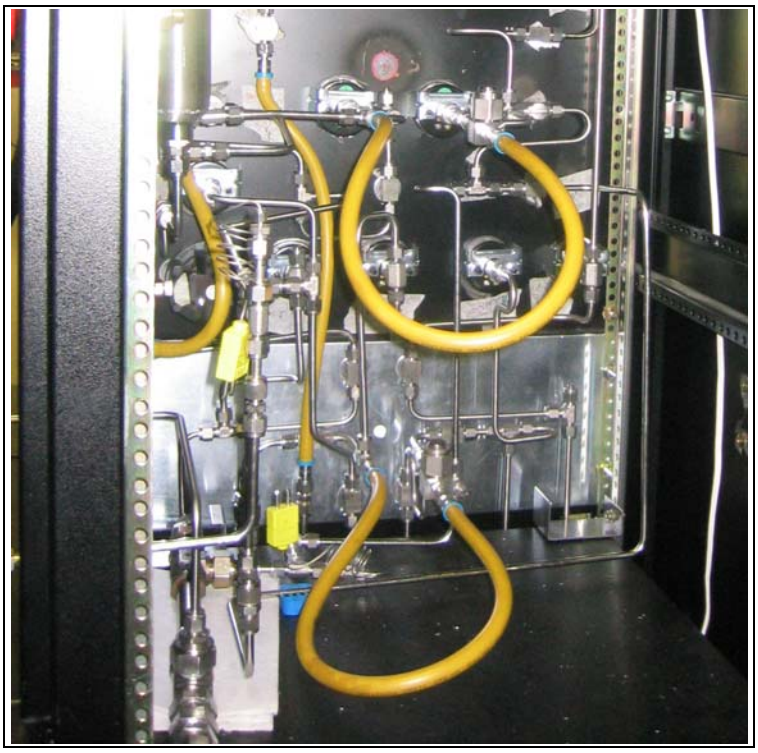

Figure 15 Test Stand - Hoses bypass points where the stack is installed

4.3.2 Thin section, Photoetched Corrosion Resistant Components

The use of photoetched parts was explored by Analytic in its contract with the USMC to build EHCs. The parts were fabricated from (316) stainless steel. We proposed to use photo etched molybdenum, niobium or 316 SS parts. The use of these components eliminates the relatively thick components (and flow fields) of our prior designs. This permitted a cell pitch in excess of 33 cells/inch. Unfortunately, the etching process proved expensive and the material were likewise. Corrosion of the parts was a severe problem.

4.4 Organization of the program

To implement the design changes, the program tasks were designed as follows:

4.4.1 Design

4.4.1.1 Unit Cell

The Unit cell was redesigned to accommodate the hydraulic cathode and the thin phototeched parts. The design yielded a revolutionary approach to photoetching the bipolar plate and significant drop in the number of components per unit cell

4.4.1.2 Test stand

The test stand design resolved problems with the hydraulic cathode by combining the cooling water and the high pressure hydrogen gas. A phase separator was included in the test stand design. The design of the test stand first required redesigning a computer simulation code of the system so we would know the range of operating conditions that existed in the normal operation. It also required the design of instrumentation and controls into the test stand.

4.4.1.3 Cost Comparison

In the process of redesigning the test stand and unit cell a cost comparison of the redesigned EHC to commercial units was made. In addition, the EHC was evaluated in several commercial applications and DOE applications.

4.4.2 Fabrication

4.4.2.1 Test Stand

The test stand required redesign to accommodate the hydraulic cathode. A test stand was designed and constructed

4.4.2.2 Unit Cell

The redesigned cell was built. However, the photo etching company delivered the parts late so that only two experimental tests were performed. One shipment of parts, molybdenum bipolar plates, was received after the allotted time for the contract elapsed. We had negotiated to have photoetched molybdenum electrode supports made, but the vendor delivered bipolar plates instead.

4.4.3 Test

4.4.3.1 Shakedown

During shakedown it was found that the water pump on the cathode side could not pump more than 400 psi pressure. The power supply could not drive the cell harder than 500 ma/cm2. Otherwise the shakedown test was successful and the test stand performed as expected.

4.4.3.2 Seals

The Teflon seals performed as expected in that they sealed completely at 2000 psi.

4.4.3.3 Performance

A major portion of the program was supposed to focus on performance testing the unit cell. Late deliveries of parts allowed only two builds and so the data from the testing is limited. Both resistivity and mass transport limitations have been shown in section 4.7.

4.5 Problems Encountered

- The major problem encountered was the late delivery of photoetched parts which prevented us from conducting tests. In addition, the vendor was unable to supply several parts contracted.
- The cooling water pump used was incapabile of withstanding the high pressures of cathode operation.
- The current capacity of the power supply used to drive the EHC was too low to get to 1000 ma/cm2

- Cell catalyst layer extrusion through the metal electrode support screen suggested that the openings in the support screen were too large. As a result we interposed carbon paper between the metal support screen and the catalyst layer. This solved the support problem. Inadvertently, we forgot to use a microlayer of carbon on the catalyst side of the carbon paper and as a result we were limited to very low current densities.

4.6 Departure from Planned Methodology Assessment Impact on Project Results

The departure from the original EHC design caused delays in the acquisition of parts for the experiment. However, the new design achieved unprecedented cell pitch and a great reduction in part count.
The use of a carbon paper support layer solved the problem of cell support at high pressure, but leaving out the carbon microlayer limited the performance we could attain.

4.7 Summary of Results

4.7.1 EHC Test Fixture

Figure 17 shows the test fixture undergoing assembly and pre-test on a bench prior to being installed in the Test station. Because of the late delivery of cell components, the number of tests we were able to perform is much smaller than we originally estimated. In addition, the test fixture was improperly tapped by the machine shop causing great difficulties in assembly, tear down and reassembly. These problems are to be expected in the normal course of shakedown testing. The electrode support screen was etched with 10 micron diameter ports shown in Figure 16. There was some concern about the stiffness of the stainless steel mesh. The flow vs pressure drop tests underway showed the rigidity of the structure. However it was later shown that the cell catalyst layer extruded through the holes in the electrode support screen. This was remedied by inserting a piece of carbon paper between the catalyst layer and the metal screen. Testing showed that the cell was properly connected

Figure 17 Test fixture in assembly

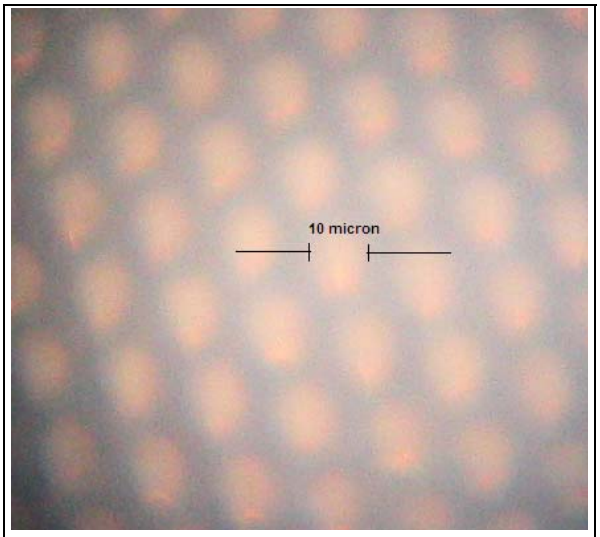

Figure 16 Electrode Support Screen Photomicrograph

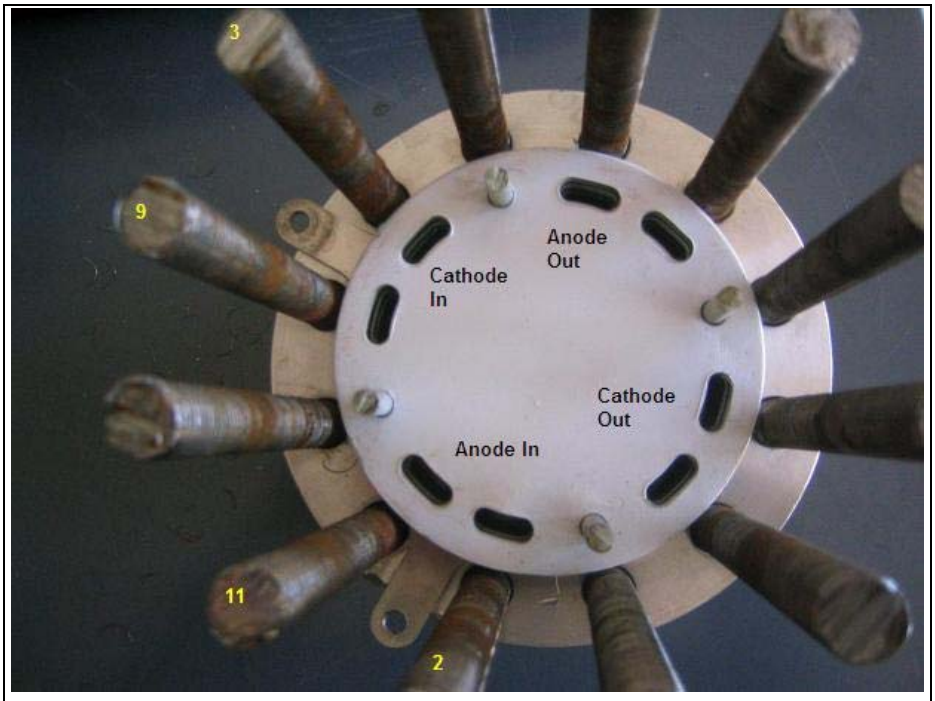

Figure 18 Test Fixture with End Plate Removed

(electrically) in the fixture. This is demonstrated by an increasing resistance when the resistance is measured with a conventional ohmmeter. Actually, the ohmmeter battery charges up the cell during this procedure. If the "resistance" appears to increase it shows that the cell has capacitance and is not shorted (or open).

4.7.2 Cell Fixture Manifolding

This section describes the flow of species through the single cell fixture. Figure 18 shows the top of the cell fixture with the anode end plates removed. The numbers 2, 11, 9 and 3 refer to the tie rod locations where the inlet manifolds are located. The cell electrical pickups are located between (2) and (11).

Removing the Anode electrical pickup plate, which is separated from the stack end plates by an insulator plate and turning the plate over, we can see the first chamber (Figure 19.) A 3 mil thick steel electrode support screen is placed on the Electrical pickup plate. Adjacent to this is a gasket and a bipolar plate with the cathode side up (facing the camera lens) as shown in Figure 20. The assembly arrangement blocks the flow of both anode and cathode

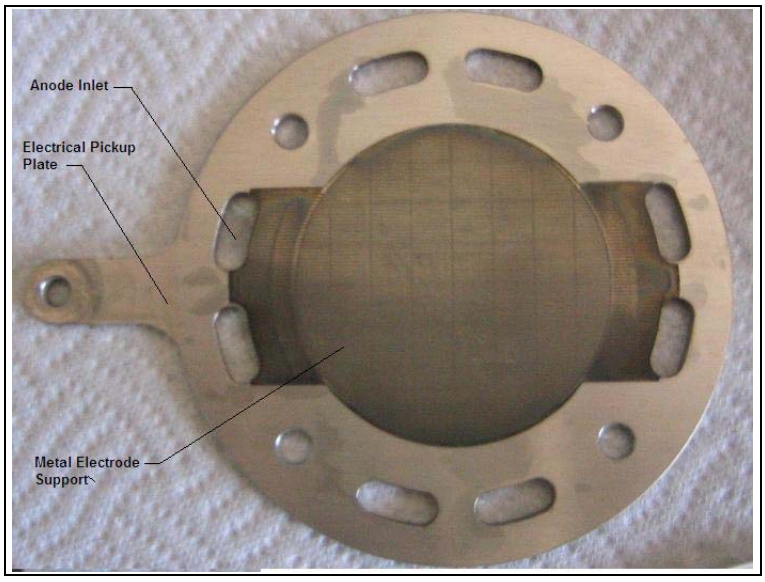

Figure 19 Dummy Anode Plate

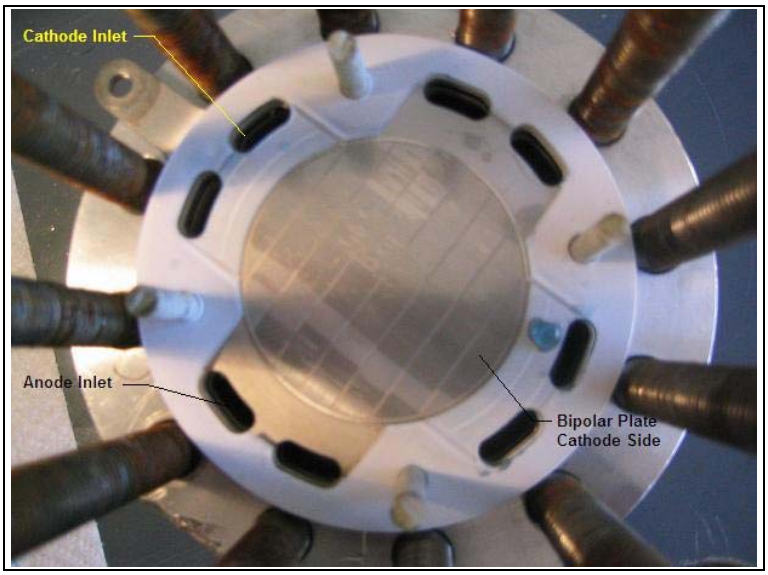

Figure 20 Cathode side of first bipolar plate

streams into the chamber formed by the first bipolar plate and the electrical conductor. The flow of anode hydrogen is blocked by the electrode support screen (Figure 19) and the flow of hydraulic cathode water is blocked by the Teflon seal which extrudes into the flow field ports as shown in Figure 20. If mixing does take place little harm would be done. At elevated cathode pressure leakage might be a concern. The fact is that an amount of water was found in the cathode flow field. The blue discoloration is indicative of some material washing out of the cathode layer. Later experiments with soaking a cell in distilled water for three days did not produce the blue discoloration. Any discoloration must have been due to the interaction of the cell catalyst layer with other cell parts during standby or operation.

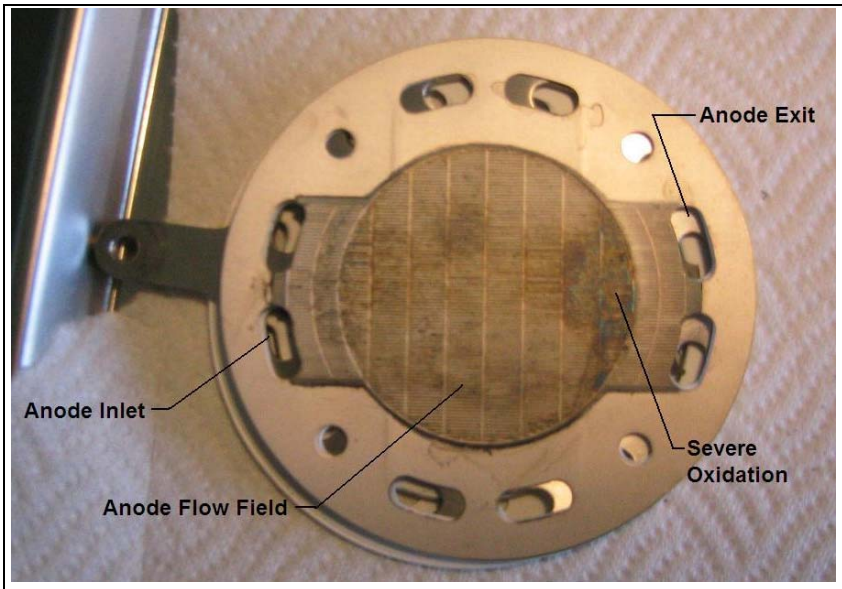

Figure 21 Anode Bipolar Plate Flow Field

4.7.3 Anode side analysis

Starting with Figure 21, which shows the Anode flow field of the Bipolar plate we examine the cell parts proper. The figure shows the oxidized state of the anode electrode support screen.

4.7.3.1 Anode Bipolar plate.

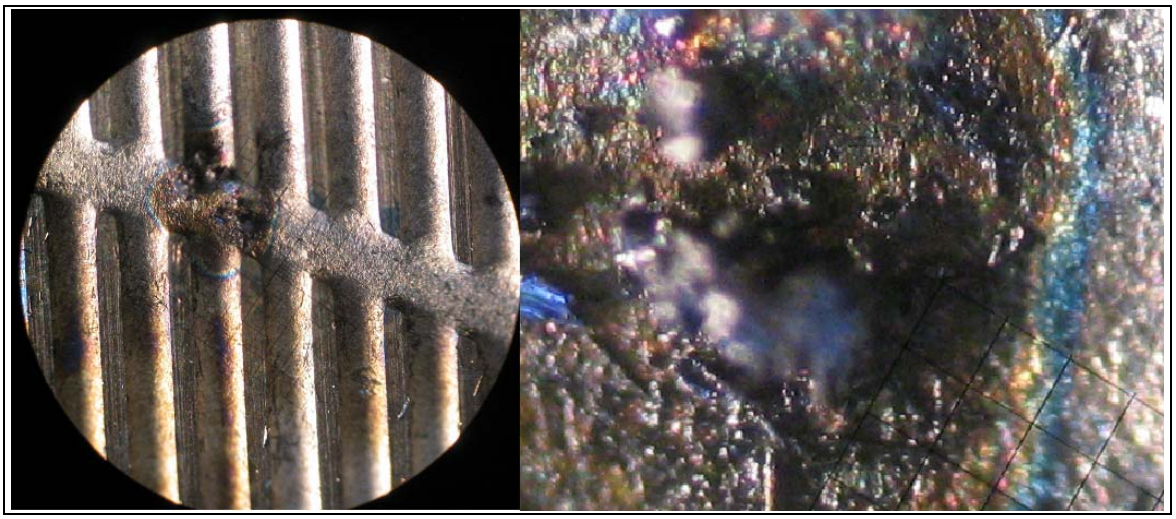

Figure 23 Flow Field Area of Anode Bipolar Plate the right photo is taken at 40X and the left is 100X.

Figure 22 Bipolar Plate - seal area 40X and 400X shows the seal area of the bipolar plate facing the Anode. The seal area showed little corrosion, however the effects of etching at 400X are evident. The roughening of the surface by the etching process makes the surface reactive. While it is likely that some components of the 316 SS alloy are etched more rapidly than others, it is not possible to say what the surface composition is.

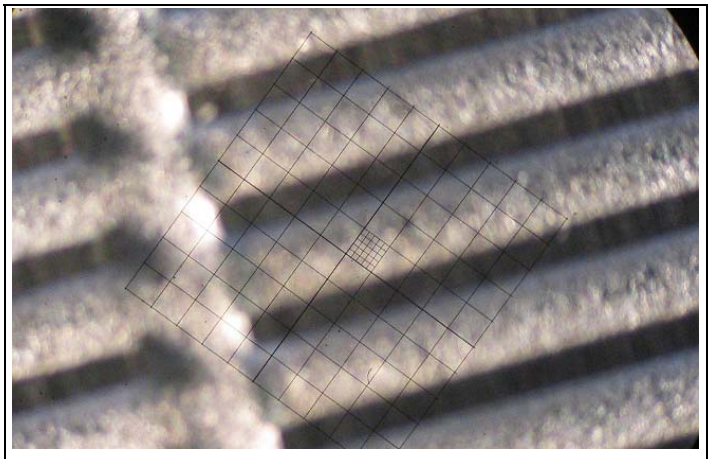

Figure 24 Dummy cathode side of Bipolar Plate 40X shown in Figure 22. Note freedom from corrosion.

The problem of corrosion is first illustrated in the Anode flow field part of the bipolar plate. The Bipolar plate is an etched structure. The bipolar plate anode flow field experiences potentials above the cathode potential. Corrosion is evident in **Error! Reference source not found.**. However, it appears to be highly localized. In general the contact surface, or "lands," of the flow field are affected, not the grooves. In Figure 24 we show the bipolar plate cathode flow field, away from the Anode. This side is free of corrosion.

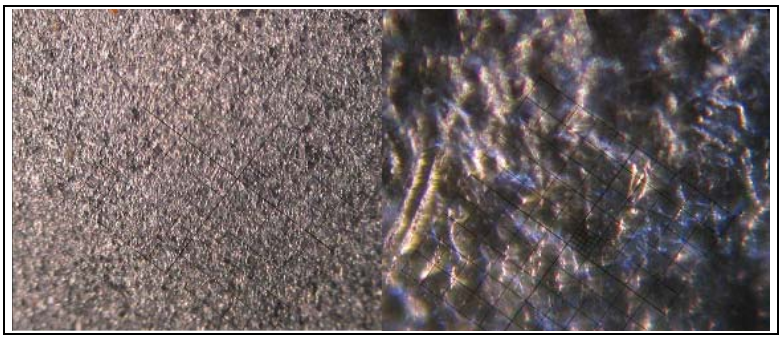

Figure 22 Bipolar Plate - seal area 40X and 400X

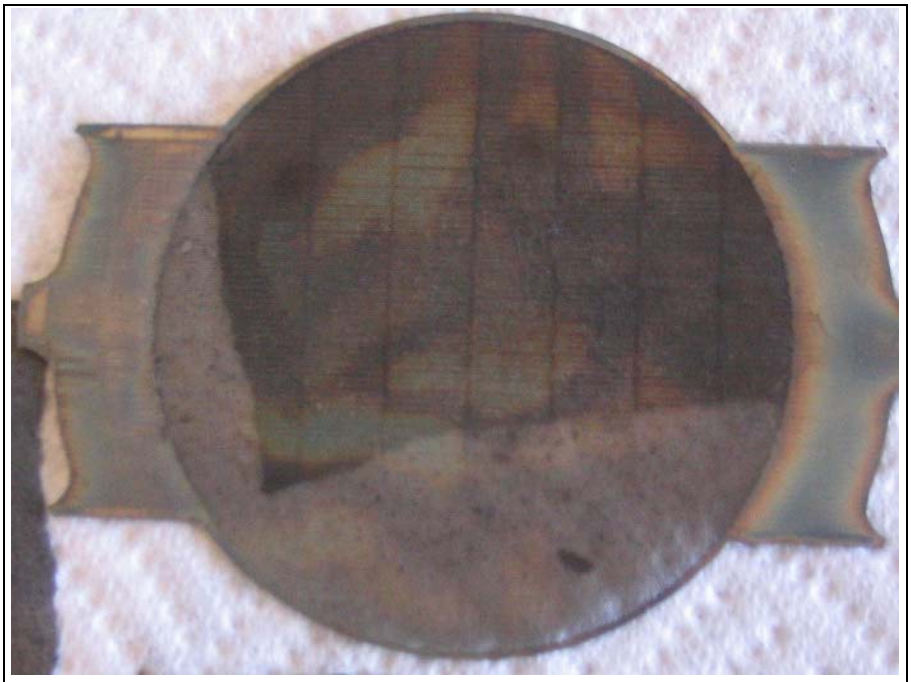

Figure 25 Anode electrode support

4.7.3.2 Anode Electrode

Figure 26 Photomicrograph anode carbon paper , gas side

The Anode electrode consists of a piece of pitch based carbon paper that had been pretreated to be hydrophobic and an etched 316SS foil. The purpose of the foil is to support the carbon paper over the flow field grooves in the bipolar plate. The carbon paper after operation was 8.5 mil thick.

In Figure 25 we show the anode support structure with the foil side up. The screen is severely oxidized in the region of the ports which show a color change indicating that the oxide formed is on the thickness of the wavelength of visible light (400 to 700 nm). The function of the anode electrode is to support the cell when large cathode pressures are developed during operation. The successful operation of the cell depends on the structural strength and corrosion resistance of the anode electrode. The anode must be thin and porous and hydrophobic. The ideal anode presents a minimum diffusion resistance for hydrogen gas flowl. Prior experience with sintered a Ti structure showed that the relatively thick sinter filled with water and obstructed the hydrogen access to the electrode. The sinter had been coated with TiN however that oxidized as well. The anode must remain oxide free to obtain a high electrical conductivity for electrons. The pores must remain clear of water, which could otherwise present diffusion problems.

In Figure 26, the membrane side of the anode is shown as a continuous smooth, carbon paper surface. Figure 27, by contrast, shows the opposite side of the carbon paper, which faces the etched, metal anode support. The figure at low magnification, shows the regular pattern of the etched metal impressed on its surface. Under high cathode pressure conditions, the anode carbon paper is extruded into the metal support layer. At the right

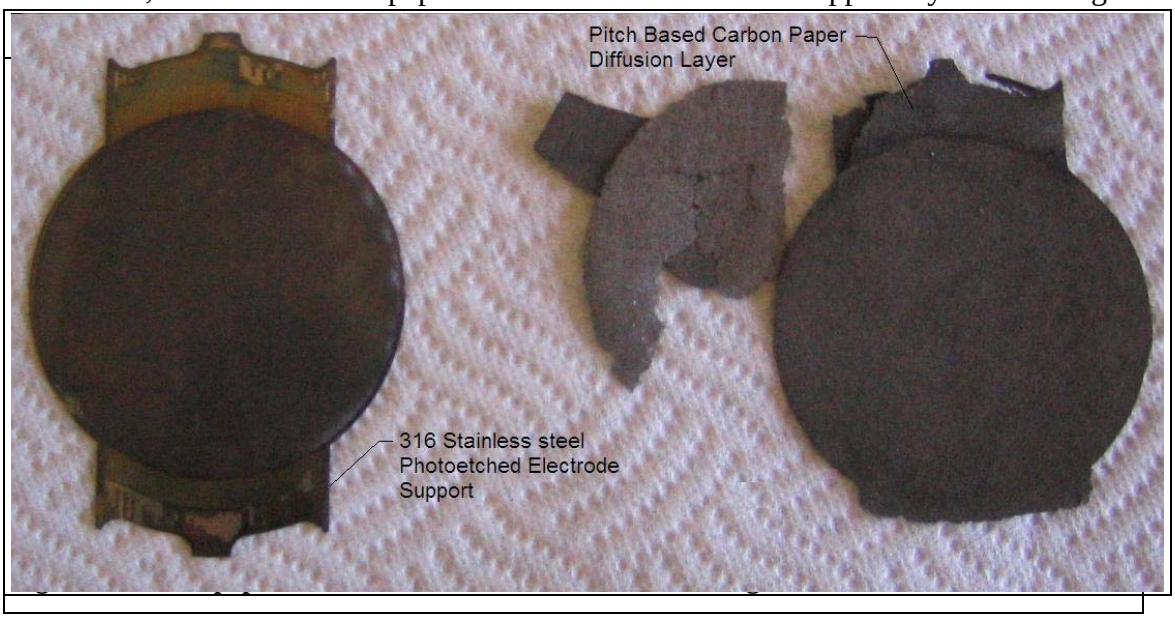

Figure 28 Cathode Electrode Structure at Teardown

side of Figure 27, it is shown that the carbon paper retains its porosity after the extrusion process. This is structurally superior to the first build of the EHC where the metal support was placed adjacent to the cell catalyst layer (Figure 16). When the cathode is pressurized in that case, the cell extruded through the openings in the metal support mesh.

4.7.4 Cathode Side

The Cathode construction is very similar to the anode. The disassembled cathode is shown in Figure 28. The cathode side of the cell is subject to a different set of stresses than the anode. The carbon paper interposed between the photoetched, 316 SS electrode support and the cell was a pitched based fiber type and electrochemically oxidized to render it hydrophyllic. The pitch based carbon paper is slightly stronger than the PAN based (Toray) fiber type used on the anode. It is not subject to the heavy compressive load to which the anode material is subject. Because the cathode cavity is filled with water, the hydrogen is formed as bubbles. The bubbles mechanically stress the carbon paper as they escape into the hydraulic cathode coolant water. The stresses have delaminated the carbon paper diffusion layer between the cathode electrode and the metal cathode support. A delaminated piece is shown in Figure 28

Figure 29 Oxidation in the Cathode Port showing imprint of bipolar plate flow field lands

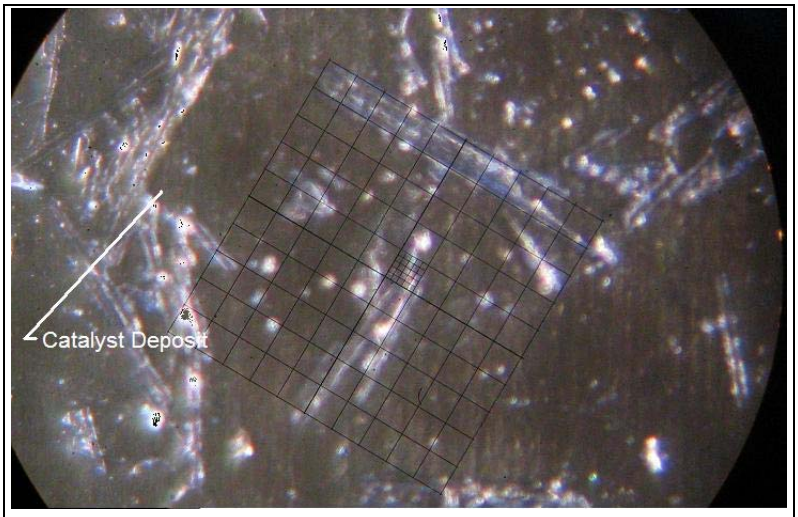

Figure 30 Catalyst may have moved in the EHC cathode

It was noted in the first build and in the second build of the cell that the cell itself released a blue color into the water and may have also released catalyst as well. The blue colored water is shown in Figure 20. In the photomicrograph shown in Figure 30 , some catalyst deposit along the metal electrode support, exit port trailing edge. Separate test were conducted on the cell showing that immersion in distilled water did not cause the release of a blue color. Some as yet unidentified fuel cell/hardware interaction must be occuring.

4.7.4.1 Cathode Corrosion

The cathode may have experienced severe oxidation. The conclusion here is tentative because the color appears to be brown in Figure 28. Figure 29, shows the oxidation of the metal electrode support in the port region. The imprint of the lands of the bipolar plate flow field are shown as unoxidized metal. The oxidation takes place at all points in

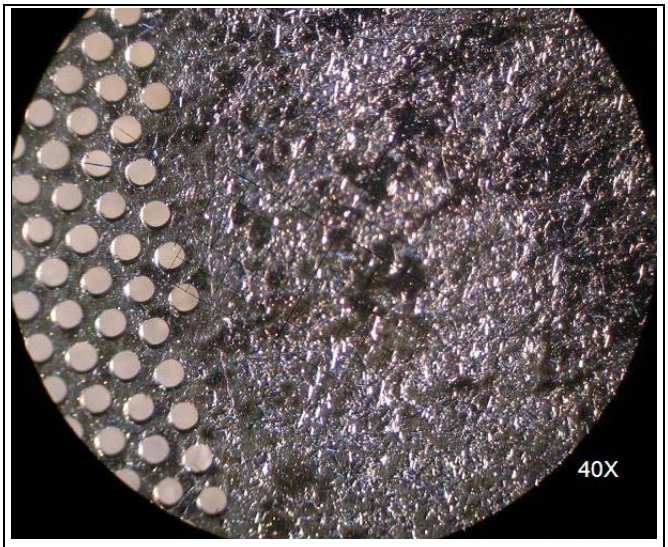

Figure 31 Cell Side Metal Electrode Support 40X

contact with water except at points which contact the flow field lands. The pattern of oxidation is reversed along the flow path to the active area of the cell. The flow field imprint does not show on the opposite side (cell catalyst side) of the electrode support, which is in contact with the carbon paper. Here the oxidized layer is relatively smooth. The side of the perforated electrode support adjacent to the bipolar plate shows a relatively smooth surface which may be brownish from an oxide layer or it may be colored brown from electrocatalyst deposit, or some organic oxidation product. The side facing the carbon paper, Figure 31 showed both black deposits and oxidation effects.

Table 9 Resistivity (ohm-cm^2) Build 2 Components

Pressure psi	As Built Cell	Dummy Anode	Bare cathode	Cathode & Cpaper	Anode & Cpaper
400	1.174	0.106	0.503	0.555	0.142
1000	1.084	0.000	0.219	0.168	0.093

4.7.5 Resistivity Measurement

The formation of oxide layers on the cell components and fixture appears to be an important phenomenon associated with the operation of the cell, even if the operation was brief. A series of measurements were made of the electrode, supports and cell. These measurements are done using an Analytic Power fixture. Resistance measurements are taken with an HP4328a milliohmmeter. Samples are placed between Toray carbon paper platen covers, and the resistivities are recorded at 0, 400 and 1000 psi. The results are shown in Table 9

Table 10Comparative Resistivities (ohm-cm2) with microlayers

Pressure psi	Nafion 117 Cell	Build 1 Cathode	Anode Screen	Anod (Rev Cpaper)	Bipolar Plate
400	0.660	0.041	0.764	1.331	0.299
600	0.645	0.052	0.464	0.800	0.181
1000	0.604	0.036	0.243	0.346	0.152

The formation of oxide layers on the cell components and fixture appears to be an important phenomenon associated with the operation of the cell, even if the operation is brief. A series of measurements were made of the electrode, supports and cell.
For comparison purposes we made several measurements, Table 10, which are helpful in diagnosing whether the performance problems are attributable to resistivity. These

measurements were made with Analytic Power gas diffusion layers (with microlayers) rather than Toray carbon paper between the components and the hardware platens. The cell has a notably lower resistance when the carbon paper used had a carbon microlayer.

4.7.5.1 Electrodes

In Table 9 and Table 10 the resistivities show the benefits of carbon paper for lowering the resistance. The Figure 32 values are obtained with the as built carbon paper in place

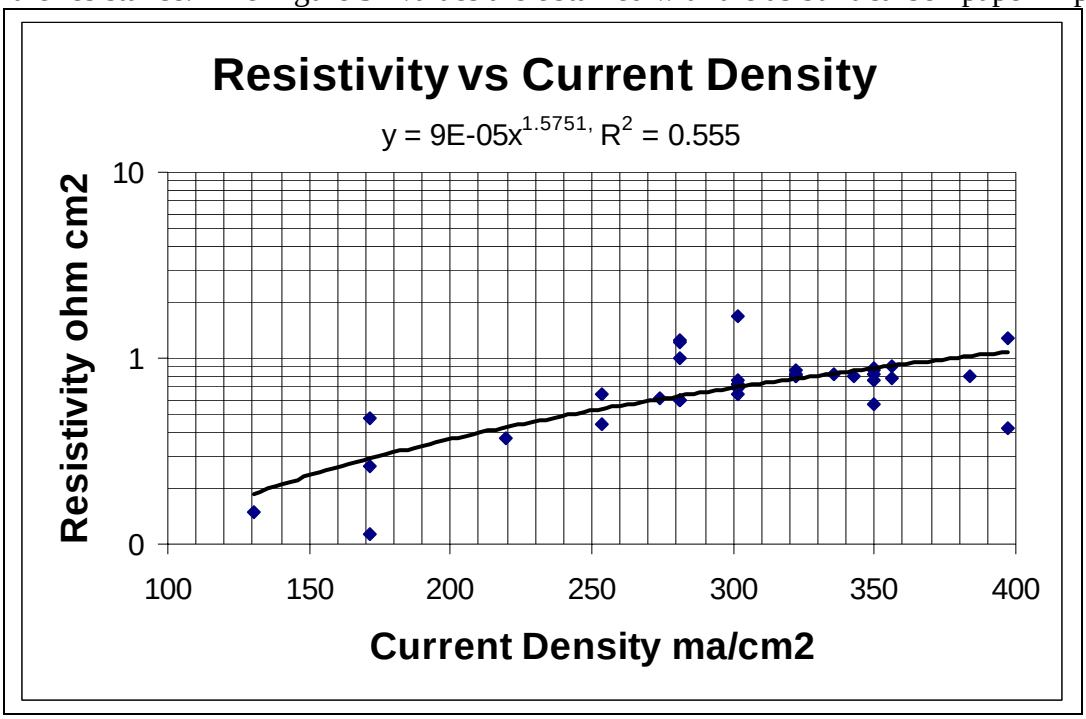

Figure 32 Resistivity Measurements of Build 2 follow a power law in current density

next to the stainless steel support screen. The important point, however, is to compare the Build 1 cathode and the anode screen with the GDL microlayers adjacent to the screen, and reversed. These columns clearly show the effect of the highly oxidized surface of the Build 2 anode screen on resistivity as well as the effect of placing the harder surface of the reversed carbon paper adjacent to the screen.

As shown in the figure, the resistivities of the build 2 electrodes (with cpaper in place) are 0.09 and 0.18 ohm-cm^2. The sum of the resistivities is 0.3 ohm cm^2. If the total polarization of the cell is expressed as a resistivity (ohm cm2) as in Figure 32 and plotted against current density one can fit the data with a power law expression. This indicates the presence of electrochemical kinetics effects, and even a mass transport component

4.7.5.2 Cell

The used cell was removed from the test fixture and immersed in distilled water for three days. It was then subjected to resistance measurements identical to those used for measuring other cell component resistances. The cell resistance was measured and found to be 56 mohm at 400 psi contact pressure and 52 mohm at 1000 psi. Subtracting the hardware resistance of 10mohm, this yields a resistivity of 1.084 ohm cm^2. 1100 EW

Nafion has an areal resistivity of 0.07 to 0.16 ohm cm^2. An order of magnitude increase in resistivity, has occurred, which may be attributed to:

- catalyst layer resistance,
- corrosion of the stainless steel cell components.

Generally, if corrosion products are formed at either electrode, the polyvalent, transition

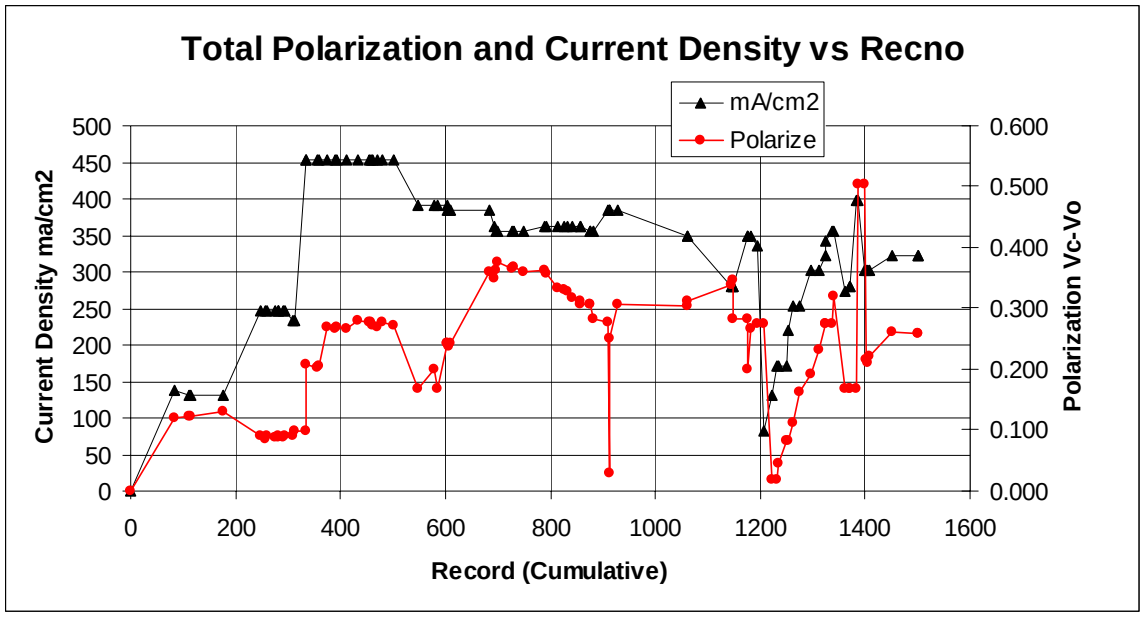

Figure 33 Build No. 2 Histogram (Recno equals Record Number)

metal cations will accumulate in the membrane. Initially, these ions reduce the limiting current. If concentrated in massive amounts, the cell resistance will increase. The cells have not been titrated to determine the membrane equivalent weight, yet. For comparative purposes, a fresh Nafion 117 cell (the original was a Nafion 112 mea) was soaked in distilled water and its resistance measured, as shown in Table 10, is about 80% lower than the Build 2 cell.

4.7.6 Cell Performance

The individual component resistivities: anode, cathode and cell sum to 1.345 ohm cm2. Based on these resistivities, it would have been impossible to attain the performance level demonstrated by the cell. The cell performance was obtained on 3/15/06 most likely, the component resistances increased subsequent to that, or at least on teardown the resistivities increased. Figure 33 shows the relationship between the current density and the total polarization expressed as a histogram of the first three data collection runs. The record numbers for the first run are between 0 and 177, for the second run they extend from 247 to 501. Data for the third run were collected for record numbers above 501. The data were taken at several pressures. The total polarization was expressed as the measured cell voltage less the change in Nernst potential (ΔV) due to the pressure ratio. The figure shows that the polarization follows the Nernst Relationship.

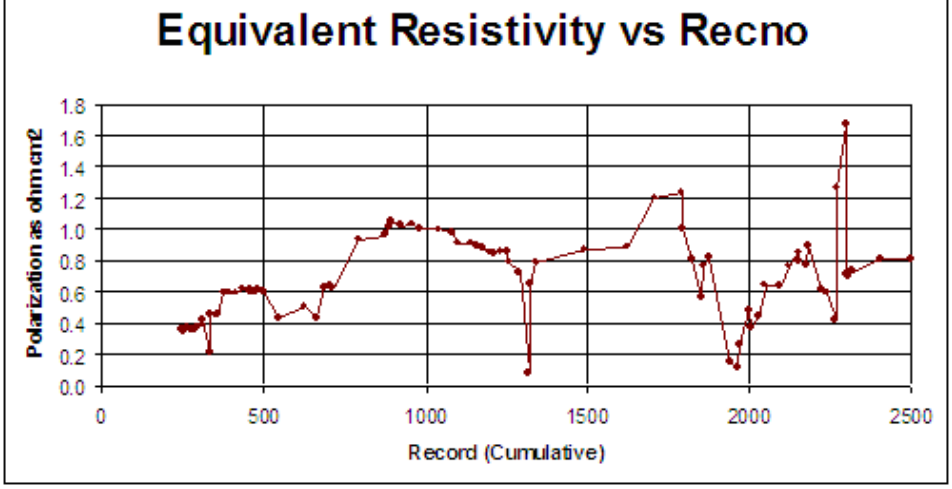

Figure 34 Total Polarization expressed as a Resistivity

$\Delta V = RT/nF \ln(rp)$ Nernst

In Figure 34 we combine the polarization in volts with the current density along with the cell area to express the polarization as a resistivity term. The results showed that the resistivity is not a constant and must have been lower than the measured value at teardown. If we assume a resistivity of ~0.2 ohm cm2, we obtain the results shown in Figure 35. In this diagram, below 20 ma/cm2, the voltage vs current density is given by the Tafel-like expression:

$$Vc=0.143+0.113\ln(J/200)$$

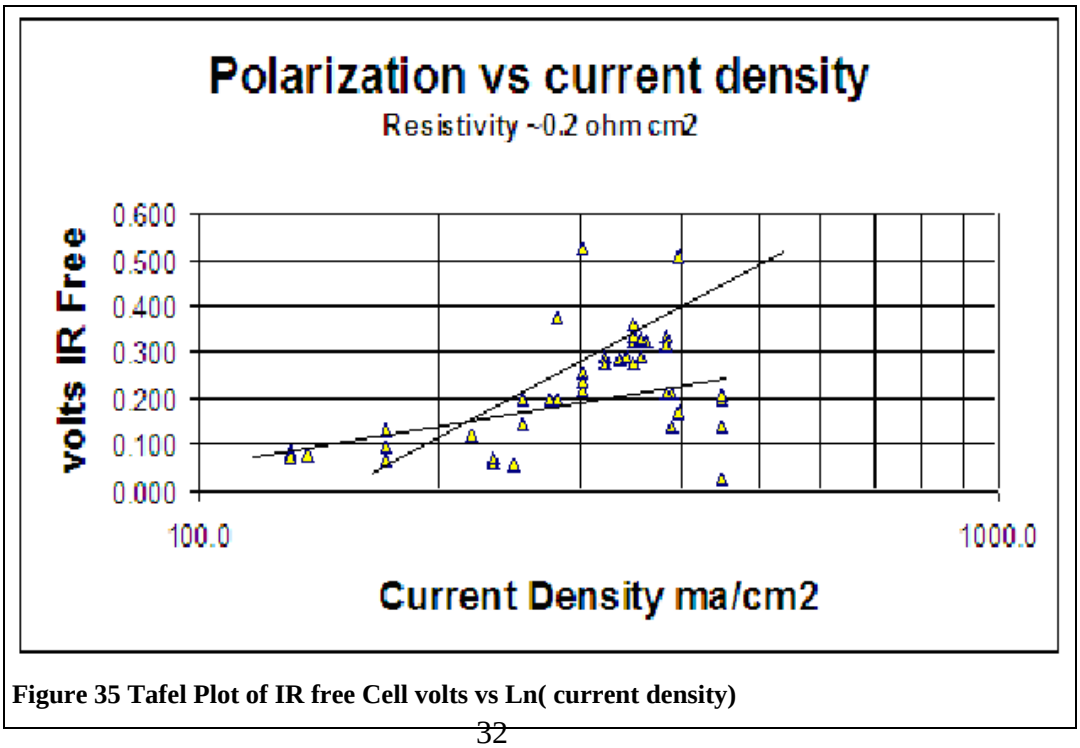

Figure 35 Tafel Plot of IR free Cell volts vs Ln(current density)

Where the Tafel slope (b=0.113) represents catalyst kinetic polarization. Above 200 ma/cm2, the relationship is given by \:

Vc= 0.1029-0.429Ln(200/J)

The slope of the line has increased by a factor of 3.8 indicating that above 200 ma/cm2, the cell performance is strongly mass transfer limited. While it appears that the anode structure is open, something blocked the entry of hydrogen into the catalyst layer.

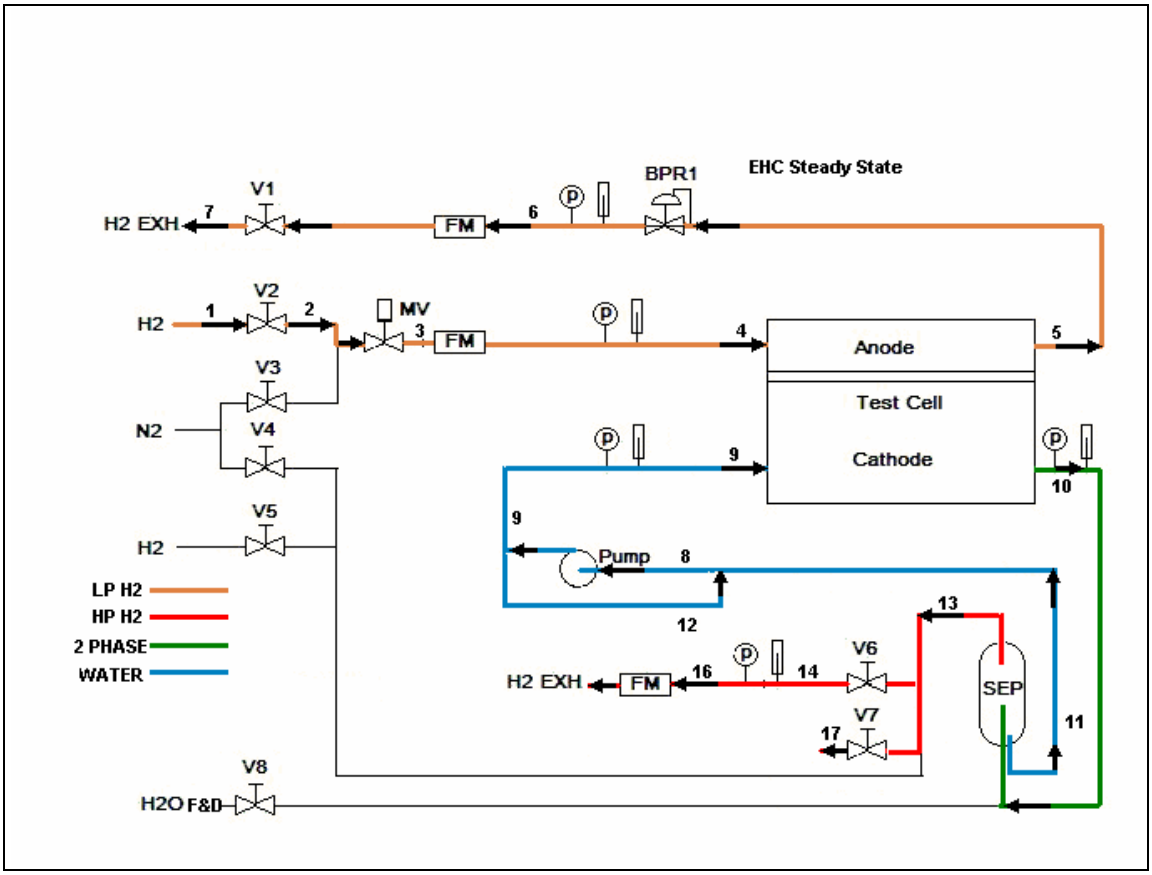

Figure 36 Test Stand Schematic Diagram

Table 11 Glossary to the Node Array

Temperatuire	– F	T(N)
Pressure	- Atm	P(N)
Flow rate	- lb mole/hr	H2(N), H2O(N),
Enthalpy	- Btu/hr F (total rather than specific)	H(N)
Entropy	- Btu/F (total rather than specific)	S(N)
Heat capacity	- Btu/F (total rather than specific)	Cp(N)
Node Number	Location (see Figure 44) in the flow schematic	N

5 PRODUCTS DEVELOPED

No Products were developed under this award.

Table 12 Max current density Node Array

EHC-FLO, 11/15/05, 1 A/cm^2								
NODE	1	2	3	4	5	6	7	8
H2	2.00E-03	2.00E-03	2.00E-03	2.00E-03	6.01E-04	6.01E-04	6.01E-04	
H2O					2.89E-04	2.89E-04	2.89E-04	1.93E-01
TOTAL	2.00E-03	2.00E-03	2.00E-03	2.00E-03	8.90E-04	8.90E-04	8.90E-04	1.93E-01
T(N)	70	70	70	70	160	160	160	170
P(N)	3.40	3.40	1.00	1.00	1.00	1.00	1.00	27.00
H(N)	7.21E+00	7.21E+00	7.21E+00	7.21E+00	-2.58E+01	-2.58E+01	-2.58E+01	-2.24E+04
S(N)	7.96E-02	7.96E-02	8.44E-02	8.44E-02	4.06E-02	4.06E-02	4.06E-02	2.98E+00
CP(N)	1.38E-02	1.38E-02	1.38E-02	1.38E-02	6.49E-03	6.49E-03	6.49E-03	3.90E+00
NODE	9	10	11	12	13	14	15	17
H2		1.40E-03			1.40E-03	1.40E-03	1.40E-03	1.40E-03
H2O	1.93E-01	1.93E-01	1.93E-01	1.93E-01	1.71E-05	1.71E-05		
TOTAL	1.93E-01	1.94E-01	1.93E-01	1.93E-01	1.42E-03	1.42E-03	1.40E-03	1.40E-03
T(N)	170	170	170	170	170	170	170	170
P(N)	27.0	27.0	27.0	27.0	27.0	1.0	1.0	1.0
H(N)	-2.24E+04	-2.24E+04	-2.24E+04	-2.24E+04	4.34E+00	4.34E+00	6.01E+00	6.01E+00
S(N)	2.98E+00	3.03E+00	2.98E+00	2.98E+00	5.24E-02	6.16E-02	6.08E-02	6.08E-02
CP(N)	3.90	3.91	3.90	3.90	0.01	0.01	0.01	0.01

Table 13 Min Current Density Node Array

EHC-FLO, 11/15/05, 01 A/cm2								
NODE	1	2	3	4	5	6	7	8
H2	2.00E-04	2.00E-04	2.00E-04	2.00E-04	6.01E-05	6.01E-05	6.01E-05	
H2O					2.89E-05	2.89E-05	2.89E-05	1.93E-02
TOTAL	2.00E-04	2.00E-04	2.00E-04	2.00E-04	8.90E-05	8.90E-05	8.90E-05	1.93E-02
T(N)	70	70	70	70	160	160	160	170
P(N)	3.40	3.40	1.00	1.00	1.00	1.00	1.00	27.00
H(N)	7.21E-01	7.21E-01	7.21E-01	7.21E-01	-2.58E+00	-2.58E+00	-2.58E+00	-2.24E+03
S(N)	7.96E-03	7.96E-03	8.44E-03	8.44E-03	4.06E-03	4.06E-03	4.06E-03	2.98E-01
CP(N)	1.38E-03	1.38E-03	1.38E-03	1.38E-03	6.49E-04	6.49E-04	6.49E-04	3.90E-01
NODE	9	10	11	12	13	14	15	17
H2		1.40E-04			1.40E-04	1.40E-04	1.40E-04	1.40E-04
H2O	1.93E-02	1.93E-02	1.93E-02	1.93E-02	1.71E-06	1.71E-06		
TOTAL	1.93E-02	1.94E-02	1.93E-02	1.93E-02	1.42E-04	1.42E-04	1.40E-04	1.40E-04
T(N)	170	170	170	170	170	170	170	170
P(N)	27.00	27.00	27.00	27.00	27.00	1.00	1.00	1.00
H(N)	-2.24E+03	-2.24E+03	-2.24E+03	-2.24E+03	4.34E-01	4.34E-01	6.01E-01	6.01E-01
S(N)	2.98E-01	3.03E-01	2.98E-01	2.98E-01	5.24E-03	6.16E-03	6.08E-03	6.08E-03
CP(N)	3.90E-01	3.91E-01	3.90E-01	3.90E-01	9.82E-04	9.82E-04	9.68E-04	9.68E-04

6 COMPUTER MODELING

A computer model of the EHC was constructed in order to size components and to assess the values of temperatures, pressures and flows throughout the test stand during normal operation

The schematic diagram in Figure 36 shows the location of all major components, instrumentation and node numbers throughout the test stand. Node arrays of the data generated by the simulation program are shown in Table 12 andTable 13. SAE units are used. As shown in the Glossary of Table 11.

The simulation program is a Q Basic program written by Analytic. It has been used in virtually all Analytic Power contracts over a twenty year period. The program has been used by commercial customers in the US and abroad as well as DOE and DOD.

The Performance criteria used is based on prior Electrochemical Compressors built by Analytic.
Test results to demonstrate the model performance criteria were not met because of very low performance of the single cell tested. The bulk of the performance problem lies in the rapid corrosion of cell components used.

MicroFlo Q&A

Theory behind the model, expressed in non-mathematical terms;
The MicroFlo Model is a linear, sequential, modular systems analysis code.

Mathematics to be used, including formulas and calculation methods;
The documentation of the model completely describes MicroFlo and has been supplied to DOE on occasion when it was developed.

Whether or not the theory and mathematical algorithms were peer reviewed, and, if so, include a summary of theoretical strengths and weaknesses;
The model has been commercially available for over twenty years and has been used by DOE, and DOD.

Hardware requirements; and Documentation (e.g., users guide, model code).
The model runs on any microcomputer equipped with Windows and Q Basic (a Microsoft Product) the system runs under DOS.